Electrokinetic Perfusion Through 3D Culture Reduces Cell Mortality

Anyesha Sarkar PhD¹ and Mark A. Messerli PhD¹

¹Department of Biology and Microbiology, South Dakota State University, Brookings, SD, 57007

Running title: electrically driven interstitial flow

Keywords: electrokinetic perfusion, extracellular matrix, cell viability

Corresponding Author:

Mark A Messerli PhD 1390 North Campus Drive SNP 252, Box 2140D South Dakota State University Brookings, SD 57007 Mark.Messerli@sdstate.edu 605 688-5667

Anyesha Sarkar 1390 North Campus Drive SNP 252, Box 2140D South Dakota State University Brookings, SD 57007 Anyesha.Sarkar@sdstate.edu 605 688-5493

Abstract

Cell proliferation and survival are dependent on mass transfer. *In vivo*, fluid flow promotes mass transfer through the vasculature and interstitial space, providing a continuous supply of nutrients and removal of cellular waste products. In the absence of sufficient flow, mass transfer is limited by diffusion and poses significant challenges to cell survival during tissue engineering, tissue transplantation and treatment of degenerative diseases. Artificial perfusion may overcome these challenges. In this work, we compare the efficacy of pressure driven perfusion with electrokinetic perfusion toward reducing cell mortality in 3D cultures of Matrigel extracellular matrix. We characterize electro-osmotic flow through Matrigel to identify conditions that generate similar interstitial flow rates to those induced by pressure. We also compare changes in cell mortality induced by continuous or pulsed electrokinetic perfusion. We report that continuous electrokinetic perfusion significantly reduced mortality throughout the perfusion channels more consistently than pressure driven perfusion at similar flow rates, and pulsed electrokinetic perfusion decreased mortality just as effectively as continuous electrokinetic perfusion. We conclude that electrokinetic perfusion has significant advantages over pressure driven perfusion for promoting tissue survival prior to neovascularization and angiogenesis.

Impact Statement

Interstitial flow helps promote mass transfer and cell survival in tissues and organs. This study generated interstitial flow using pressure driven perfusion or electrokinetic perfusion to promote cell viability in 3D cultures. Electrokinetic perfusion through charged extracellular matrices possesses significant advantages over pressure driven perfusion and may promote cell survival during tissue engineering, transplantations, and treatment of degenerative diseases.

Introduction

Mass transfer is one of the greatest challenges to tissue engineering. ^{1,2} *In vivo*, mass transfer is performed mostly through blood and lymphatic vessels, and to a lesser extent, interstitial flow occurs in the extracellular space. ³ These forms of fluid flow enhance cellular exposure to gases, nutrients, and growth factors while removing metabolic wastes, cellular detritus, and death signals. Challenges with mass transfer are also associated with degenerative diseases and during tissue transplantation when sparse or damaged vessels limit repair and regrowth. ^{2,4,5} These challenges might be overcome with artificially generated interstitial flow to promote cell survival during periods of neovascularization and angiogenesis that are required for tissue survival.

In the absence of flow, mass transfer is a limiting factor in cell culture when mortality most commonly occurs through apoptosis in response to hypoxia, metabolically induced low pH, or low growth factors.^{6,7} Starvation can cause autophagy⁸ and more severe physical and chemical stresses can promote necrosis⁶. Artificial perfusion of media as low as 0.07 μm/s is reported to overcome diffusion limitations in 2D culture and increase cell proliferation by 40%.⁹ While pressure promotes perfusion through 3D cell cultures, it also causes compaction of the tissue and increases hydraulic resistance.^{10,11} Charged hydrogels that mimic the native extracellular matrix show greater hydraulic resistance to physiological saline compared to neutral gels.¹² Moreover, pressure driven perfusion (PDP) is limited by drag. According to Poiseuille's Law, average flow velocity changes with the square of the distance between the walls of a particular pathway. Given the same pressure gradient across a tissue (Δpressure / length), narrow pathways in the tissue have greater resistance to flow and slower flow velocity than larger diameter pathways with lower resistance and faster flow. Therefore, flow velocity through narrow pathways is slow and may be insufficient to promote survival, while the velocity through wider pathways is faster and may damage cells through shear stress. These limitations of pressure driven perfusion may be overcome using electrokinetic perfusion (EKP).

Applied electric fields (EFs) through isotropic, charged gels generate electro-osmotic flow (EOF) and electrophoresis without gel deformation. ^{13,14} In 2D culture, applied EFs generate EOF within nanometers of the boundary layer of cells, sufficient to redistribute surface macromolecules within minutes and activate mechanosensitive ion channels via shear stress. ¹⁵⁻¹⁷ In 3D tissues, relatively weak EFs generate EOF that is comparable in speed to endogenous velocities of interstitial flow, 0.1-2 μm/s, ^{3,18-20} EOF velocity is more uniform in narrow pathways where PDP is limited by drag. In 3D culture, we hypothesize that EKP will help cells overcome diffusion limitations and reduce cell mortality. To test this hypothesis, we have induced interstitial flow through 3D cultures in Matrigel, using pressure or electricity. We controlled the average interstitial flow rates in the gels and compared efficacy of the two methods in reducing cell mortality. Our results indicate that steady and intermittent EKP generate interstitial flow and reduce cell mortality.

Materials and Methods

Measurement of electro-osmotic flow

EOF through Matrigel (Corning, New York) that was cast in IBIDI channel slides (IBIDI μ-slide VI 0.4 Collagen IV), was measured at ambient temperature in experimental media by tracking the dye front of neutral Texas red dextrans (3, 10, or 70 kDa). Microbial transglutaminase (Moo Gloo RM Transglutaminase, Modernist Pantry) at a final concentration of 100 μg/ml was used to crosslink Matrigel in modified Ringer's (MR) to provide strength. Addition of the transglutaminase solution diluted Matrigel to 88%. The dye front of Texas red dextran (ex./em. 595/615 nm) was tracked in the presence of DC EFs (Lambda Electronics Inc., Melville, N.Y.) and pulsed EFs using a 611 stimulator (Phipps and Bird, Inc. Richmond, VA) for 50% duty cycle and an arbitrary function generator (AFG 3021, Tektronix, Inc., Portland, OR) controlling a voltage amplifier (Model MDT693, Thorlabs Inc., Newton, NJ) for 25% duty cycle. Time-lapse images of the dye front were acquired using an Olympus FV1200 Confocal system with an IX81 inverted microscope. A MATLAB script (MathWorks, Natick MA) was used to track the dye front in successive frames and calculate the net flow velocity. EOF was calculated by subtracting the velocity of the dye in the absence of EFs from the velocity of dye in the presence of EFs. More details are provided in the Supplemental Information. Statistical significance was determined using unpaired t-tests.

3D Culture

Chinese hamster ovary (CHO) cells, cultured in phenol-red free Dulbecco's Modified Eagle's Medium (DMEM) with 10% FBS and 1% Pen-Strep were concentrated and mixed with the Matrigel stock. Prior to mixing, cell counts were made with a hemocytometer (Fisher Scientific) enabling determination of a final cell density of ~4.5x10⁷ cells/mL or approximately 8% by volume. The mixture of Matrigel, cells, and transglutaminase was loaded into IBIDI channel slides and allowed to gel at room temperature for 10 min. before transferring to a 37°C CO₂ incubator to complete crosslinking for 2 hours. The final Matrigel dilution is estimated to be near 54% of its original concentration._Transglutaminase in MR was added to

the channel wells to promote crosslinking at the gel edges. After crosslinking, transglutaminase was rinsed from the gels with two volumes of experimental media using EOF at 1000 mV/mm for ~40 minutes each time.

Cell assays in 3D culture

Cell mortality was assessed after 48 hours in the absence of perfusion (control) and in the presence of PDP or EKP. Mortality was monitored using the cell-impermeant Propidium Iodide (PI, 20 µM) which stains nucleotides of apoptotic, autophagic, and necrotic cells as they lose membrane integrity.^{21,22} Disintegrated nuclei or ruptured cells would be diluted by greater than 10-fold^{23,24} and would be below the threshold of detection. Cells in 3D culture were exposed to PI using EOF as described above. Images of PI-stained cells (ex./em. 535/615 nm DNA bound) were collected 30 µm from the bottom of the channels using an optical section $14.5 \pm 4.6 \,\mu m$ thick with the confocal system described above. ImageJ software was used to measure the percent area of the field of view that was covered by PI stain. Three regions of each channel were sampled twice near the inlet, center, and outlet regions to assess PI staining throughout the channel. Six channels total from at least two different experiments were used for each of the conditions that were studied. In the absence of 48 hr. perfusion, the inlet and outlet of the channel refer to the perfusion direction used to remove the transglutaminase and load the PI. For consistency, each region of the experimental channels was compared to the same region of the control channels. Relative mortality was calculated after 48 hr. as a ratio of the percent area of PI-stained cells after perfusion with the percent area of PI-stained cells from the nonperfused, control cells. The average mortality of the same batch of cells at 0 hr. was subtracted from both 48 hr. measurements. Statistical significance was calculated using unpaired t-tests.

PDP was applied through the 3D cultures with programmable syringe pumps (NE 1002X, New Era Pump Systems, Inc, Farmingdale, NY) at 300 μ L/day or 60 μ L/day, equivalent to 10 and 2 times the empty volume of the IBIDI channel. The experimental setup is described in the Supplemental Information.

Pressurized flow occasionally dislodged Matrigel so a protective low electroendosmosis (EEO) agarose gel (1%) was placed in the upstream well just before connecting the chambers to the syringes. Control experiments were performed using the same batch of cells in IBIDI channels. Both sides of control channels possessed equal volumes of CO₂ equilibrated, sterile media in tubing but the upstream syringes were not pressurized.

DC EFs at 300 mV/mm or 60 mV/mm were applied to cells using 9V battery banks. Battery banks and the pulsed power supplies were each connected to a series resistance substitution box (RS-500, Elenco, Wheeling, IL). The high series resistance was used so that applied EFs across the cells could be kept relatively constant despite subtle changes in the channel resistance. Pulsed EFs were increased by a factor of 2 and 4 for the 50% and 25% duty cycles, respectively, to maintain time averaged EFs of 300 mV/mm. More details describing the experimental setup are described in the Supplemental Information.

Velocity Profiles

To directly compare velocity profiles between PDP and EKP we modelled flow between two planes using the planar Poiseiulle equation²⁵ and equation 25 from Soderman and Jonsson ²⁶, respectively. Excel was used to calculate the pressure generated profiles and a MATLAB script was used to calculate the EOF profiles.

Results

Electro-osmotic flow through Matrigel

EOF through crosslinked Matrigel was tracked by monitoring progression of the dye front of neutral Texas Red-linked dextrans. Fig. 1A illustrates the experimental setup used to apply EOF through the Matrigel in the IBIDI channel and image movement of the fluorescent dye front. Examples of the profiles of the dye front are shown in Fig. 1B+C during exposure to 100 and 1000 mV/mm, respectively. The average movement of the dye front was determined at the steepest regions. EOF was determined for the most concentrated crosslinked Matrigel, 88%, and half its concentration, 44%, during exposure to EFs of different magnitude, Fig. 1D. The average EOF in 44% Matrigel increased from $0.6 \pm 0.1 \,\mu\text{m/s}$ at 100 mV/mm, to $1.5 \pm 0.3 \,\mu\text{m/s}$ at 300mV/mm, to $7.4 \pm 0.2 \,\mu\text{m/s}$ at 1000 mV/mm. In 88% Matrigel EOF was lower by 24%, on average, i.e. 0.4 ± 0.1 , 1.4 ± 0.1 , and $5.0 \pm 0.4 \,\mu\text{m/s}$, for 100, 300 and 1000 mV/mm, respectively, Fig. 1D.

To determine the influence of cell density on EOF velocity, similar measurements were performed through crosslinked 50% Matrigel loaded with CHO cells. EOF velocity at 1000 mV/mm did not change significantly when Matrigel was loaded with 1%, 3% or 10% cells by volume, Fig. 1E (p>0.05 for all 3 comparisons), indicating that EOF is dominated by the charge on the Matrigel macromolecules at these cellular densities.

Movement of larger neutral fluorescent dextrans was tracked to determine how well larger macromolecules could penetrate the crosslinked 50% Matrigel. The average velocity for 10 kD and 70 kD dextrans at 1000 mV/mm was significantly lower, 4.7 ± 0.3 and 5.7 ± 0.4 µm/s, respectively, than EOF for the 3 kD dextran, 8.9 ± 0.4 µm/s, Fig. 1F. We conclude that movement of the larger dextrans was impeded but still maintained relatively high mobility through the Matrigel.

In addition to continuous DC EFs, we measured EOF velocity in response to monophasic, pulsed EFs with 0.5 ms duration. Pulses with a 50% duty cycle showed an average EOF velocity of 8.4 ± 0.3 µm/s

that was not significantly different than continuous EOF, Fig. 1F. However, the 25% duty cycle showed slightly lower EOF, $6.9 \pm 0.5 \,\mu\text{m/s}$ (p < 0.01), compared with continuous EOF.

Electromigration of charged solutes

PDP generates unidirectional mass transfer while EKP generates bidirectional transfer. EKP through negatively charged gels generates both electrophoretic and electro-osmotic forces on solutes. Eq. 1 describes the sum of the forces due to electrophoresis of a solute i.e. the product of solute charge (q) and applied electric field (E), and due to electro-osmosis using Stokes' drag where solute radius (α), fluid viscosity (η), and solute velocity (ν) relative to EOF are involved. Diffusion of macromolecules through low density, porous Matrigel and low density collagen gels is similar to diffusion in water,^{27,28} therefore a correction for tortuosity is not included.²⁹

$$\sum F = qE + 6\pi\alpha\eta(EOF - v)$$
 eq. 1

During equilibrium, the sum of the forces equals zero and the velocity of the charged solute equals zero.

$$0 = qE + 6\pi\alpha\eta * EOF$$
 eq. 2

Rearranging the terms yields the relationship for the relative charge (z) to radius ratio in eq. 3, where z is the absolute charge (q) divided by the unit of charge on an electron (e).

$$\frac{z}{\alpha} = -\frac{6\pi\eta * EOF}{E * e}$$
 eq. 3

Eq. 3 describes equilibrium between electrophoresis and electro-osmosis and is useful for predicting the direction of electromigration for specific solutes. Solutes with a z/α ratio greater than equilibrium will migrate toward the cathode while solutes with a z/α ratio less than equilibrium will migrate toward the anode. The z/α ratios of representative solutes, i.e. inorganic ions, growth factors and cytokines, are plotted in Fig. 2. Surface charge of proteins was determined using relative solvent accessibility of charged residues¹⁶ and size was approximated using the Hydrodynamic Radius Converter (Fluidic Analytics Ltd, Cambridge, UK) assuming proteins were in a globular conformation.

Equilibrium between the forces of electrophoresis and electro-osmosis in 44% Matrigel is indicated by the solid black line, Fig. 2. A greater negative charge density of the extracellular matrix will make equilibrium more negative. Solutes with neutral or net positive charge will migrate toward the cathode, Fig. 2. Negatively charged solutes with a z/α ratio less negative than equilibrium will also migrate toward the cathode, e.g. cytokines IL-6 and TNF α . However, negatively charged solutes with a z/α ratio more negative than equilibrium will migrate toward the anode, e.g. Cl⁻, epidermal growth factor (EGF), proinflammatory cytokines IL-1 α & 1 β . These results indicate that EOF will dominate migration of neutral and positively charged solutes toward the cathode under physiological conditions. However, electrophoresis will dominate electromigration of negatively charged solutes toward the anode. As a result, media at both ends of the 3D culture must be replaced during EKP to maintain solute homogeneity.

Electrokinetic perfusion decreases cell mortality in 3D culture

We compared cell mortality between 3D cultures exposed to no perfusion, PDP and EKP. Cells were cultured in crosslinked Matrigel loaded into IBIDI channel slides, illustrated in Fig. 3A. PDP at 300 and 60 μL/day generated flow rates of 2.3 and 0.5 μm/s, respectively, Fig. 3B, while EKP using EFs of 300 mV/mm and 60 mV/mm generated EOF of 1.5 ± 0.4 and 0.4 ± 0.4 μm/s, respectively, Fig. 3C. The arrangement of connectors shown in Fig. 3D-E prevented a change of net fluid height and buildup of back pressure. The 300 mV/mm field strength across the Matrigel filled channel was generated using an applied voltage difference of 5.1 V and 0.7 mA, equivalent to only 3.6 mJ/s. We conclude that the temperature of the chamber was dominated by its surroundings and not the low amount of current through the gel. Neither PDP nor EKP directed mass cell migration in Matrigel, consistent with earlier reports using higher rates of pressure driven interstitial flow.^{30,31}

Cell mortality was assessed within 1.5 mm of both ends of the 17 mm long channel and in a region near the center. Mortality was assessed immediately after Matrigel crosslinking was completed (0 hr.) and used as the baseline to determine changes to cell mortality in other channels, 48 hours later, Fig. 4. Average

mortality associated with cell handling⁷ accounted for cells covering 5.4 ± 0.5 % of the sampled regions (Fig. 5, black). After 48 hours in the CO₂ incubator (Fig. 5, gray) or on a 37°C heating block (Fig. 5, white), PI-stained cells increased on average to $26.8 \pm 1.7\%$ and $24.0 \pm 2\%$, respectively.

Two perfusion rates for PDP and EKP were performed in the presence and absence of serum containing growth factors, Fig. 6. Relative mortality was assessed as the ratio of PI-stained cells of the perfused channels to the same regions of the nonperfused, control channels and compared using one-tailed t-tests, Fig. 6. The dotted line highlights normalized mortality in the absence of perfusion. PDP of serum containing DMEM at the high rate $(2.3 \mu m/s)$ was the only perfusion experiment that showed differences in mortality between the 3 regions of the chamber. Mortality was significantly reduced at the inlet (p < 0.005) that was supported by agarose, but not at the center (p > 0.1) or outlet (p > 0.4) of the channel, Fig. 6. As none of the other experiments showed statistically different mortality between the 3 regions of the chambers, the results from the three regions were combined before further analysis.

In the absence of serum, the high rate of PDP significantly reduced mortality to 0.53 ± 0.02 . Under similar conditions the higher EKP (300 mV/mm) significantly reduced mortality to 0.3 ± 0.1 and 0.50 ± 0.04 using serum-containing DMEM and serum-free DMEM, respectively. This difference in mortality supports the fact that common CHO cells are dependent on growth factors.^{32,33} Reduced mortality between PDP and EKP at the high rates in the absence of serum is not different (p > 0.5, two-tailed t-test).

At the lower rate of PDP (0.5 μ m/s), mortality was reduced significantly to 0.74 \pm 0.03 (p < 0.005) in the presence of serum but was not significantly reduced compared to controls in the absence of serum (p > 0.05). In contrast, cell mortality at the lower EKP (60 mV/mm) reduced mortality to 0.74 \pm 0.09 (p < 0.05) in the presence of serum and to 0.65 \pm 0.06 (p < 0.005) in the absence of serum and are not statistically different from each other (p > 0.4, two tailed t-test).

To test whether the increase in cell mortality was due to starvation-induced autophagy we replaced the high basal glucose level in the serum-free DMEM (25 mM) with lower glucose (5 mM). Relative mortality in serum-free high glucose conditions was not significantly different for PDP (p > 0.05) or EKP

(p > 0.7) when compared with lower glucose levels (two-tailed t-test for both). Mortality for PDP and EKP in serum-free DMEM are displayed for comparison, Fig. 7. We conclude that depletion of glucose in the dense 3D cell culture was not increasing mortality through starvation-induced autophagy.

Repeated electrical pulses of short duration are applied for long periods of time to promote healing of nonexcitable soft tissues. $^{34\text{-}36}$ We hypothesize that these intermittent EFs would generate a time averaged EKP to reduce mortality. Cell mortality from continuous EFs at 300 mV/mm was compared to intermittent EFs with 50% and 25% duty cycles using a 0.5 ms pulse duration. The electrical waveforms associated with each condition are illustrated at the top of Fig. 8. The time averaged field strength was kept constant between the DC high rate and pulsed waveforms. The 50% and 25% duty cycles significantly reduced mortality on average to 0.49 ± 0.07 and 0.56 ± 0.05 , respectively, and are not significantly different from the high rate, continuous EKP, p > 0.9 and p > 0.5, respectively.

Discussion

We report that electrokinetic perfusion through porous tissue promotes mass transfer, Fig. 1, and reduces cell mortality with significant advantages over pressure driven perfusion, Fig. 6. We hypothesize that perfusion reduced apoptosis of CHO cells by preventing hypoxia and stabilizing the culture pH.⁷ However, the high rate of PDP with serum significantly reduced mortality only on the inlet side of the chamber, while the high rate of EKP with serum reduced mortality to a significantly greater extent throughout the channel, Fig. 6. At the lower perfusion rate in the presence of serum or at the higher perfusion rate in the absence of serum, PDP and EKP showed similar reduction of mortality in these low-density matrices, Fig. 6. We conclude that the combination of greater flow velocity and serum proteins inhibited PDP from reducing mortality throughout the channel. PDP through porous materials favors the wider pathways through Matrigel, Fig. 9. However, through isotropic charged gels, EKP generates more uniform EOF over a larger range of pathway width, ²⁶ Fig. 9.

We hypothesize that the larger pathways favored by PDP, became blocked with the larger hydrophobic serum proteins. Matrigel pores range from 6 nm to ≤ 1 µm for 100-50% Matrigel ^{11,37,38} Low density lipoprotein (~22nm diameter) is known to aggregate within Matrigel and reduce hydraulic conductivity.³⁷ Other hydrophobic proteins may have the same effect. For example, serum albumin (triangular configuration with 8 nm edges³⁹) is the most abundant protein in plasma and serum, and is normally absent from interstitial fluid between cells. Albumin is known to be 'sticky', adhering to both hydrophobic and charged moieties including collagen and albumin itself.⁴⁰⁻⁴² Even though the flow pathways could become blocked with these proteins during EKP, i.e. anodal migration of BSA (Fig. 2), we hypothesize that the narrower pathways continued to allow sufficient perfusion to reduce mortality. In addition, we hypothesize that while PDP is known to cause compaction at the inlet side, it also may have caused increased stretch toward the outlet side due to an increase in blocked pathways. This effect would increase deformation of the gel and subject the cells to greater strain induced damage. Therefore porous supports may be required at both the inlet and outlet sides during PDP.³⁰ These constraints make it very challenging to apply PDP through tissues *in vivo*. However, careful placement of electrodes *in vivo*

promotes EKP through even dense brain tissue.²⁰ Additional experiments will be needed to test the efficacy of EKP *in vivo* where extracellular matrix density and net negative charge vary.

We hypothesize that electrical therapies with a time-averaged DC component, 4,34-36,43 may promote interstitial flow to promote healing and recovery of soft tissues. We tested whether short duration, monophasic pulses, commonly used during these electrical therapies, were sufficient to reduce mortality. Both pulsed waveforms, significantly reduced mortality and were not different than 300 mV/mm DC EF, consistent with a time averaged EKP. This hypothesis might be questioned for electrical therapies when electrodes are placed on top of high resistance skin. However, it is dry skin that has high electrical resistance while resistance across wet skin is an order of magnitude lower. Moreover, the resistance of electrically stimulated skin decreases by 2-3 orders of magnitude within milliseconds of stimulation. Therefore, monophasic electrical pulses, commonly applied to heal chronic epidermal wounds or promote healing of skin grafts, 47,48 lower the electrical resistance of skin and may generate time averaged interstitial flow through tissues.

EKP rescued cell viability in an EF dependent manner but we did not explore the upper limit of this phenomenon due to limitations with the current system. Addition of blood vessels has supported construction and transplantation of 2 dimensional cardiac patches ≥ 1 mm thick.^{49,50} However, in the absence of blood flow, diffusion limits tissue construction to about 0.2-0.4 mm diameter.^{1,2} We show that EKP reduced cell mortality over a distance 50 times greater and its limit has not yet been reached. In longer channels we hypothesize that nutrients will be depleted before they reach the opposite end of the chamber and that higher flow rates may extend this limit. We hypothesize that EOF could be increased 10-fold greater than used in these studies. An upper limit for artificial interstitial flow appears to be ~13 μ m/s, when pressure driven flow began to increase cell rounding and death of fibroblasts in 3D cultures.^{30,31} With respect to the upper limit for applied EFs, increased mortality of electrically excitable cells was identified in brain slices exposed to DC EFs \geq 2800 mV/mm for 5 min., while lower voltages did not increase mortality.^{51,52} This indicates that the DC EKP may be increased by nearly 10-fold before voltage-dependent

mortality is expected. Greater charge density of native extracellular matrices will enable higher EKP at lower applied EFs.

Intermittent EKP requires further investigation near excitable and nonexcitable cells. Brief, monophasic pulses require much greater amplitude to charge membrane capacitance and depolarize cell membranes. While this varies with cells and their plasma membrane time constant, our results indicate that EKP can be induced at a higher frequency that is below sensory threshold for excitable cells.⁵³ Therefore, EKP may be useful for sustaining viability during construction of electrically excitable tissues as well as nonexcitable tissues.

Conclusion

We conclude that electrokinetic perfusion through negatively charged extracellular matrices promotes interstitial flow and reduces cell mortality by preventing apoptosis. This form of perfusion has significant advantages over pressure driven perfusion especially in the narrow spaces that exist between cells *in vivo* and in 3D tissue culture. In the absence of sufficient flow through blood or lymphatic vessels, electrical therapies may stimulate healing of soft tissues by promoting interstitial flow.

Acknowledgements

We thank Dr. Michael Hildreth for maintaining equipment in the functional genomics core facility used in this work. We thank Dr. Stephen Gent for technical discussions.

Authorship Confirmation Statement:

AS and MM designed and performed the experiments, analyzed the results and wrote the manuscript.

Authorship disclosure:

The authors have no competing interests with this work.

Funding statement:

This work was supported by departmental startup funds, USDA NIFA SDSU Agricultural Experiment Station Hatch grant SD00H608-16, and NSF award #2033522 to M.A.M

Figure Legends

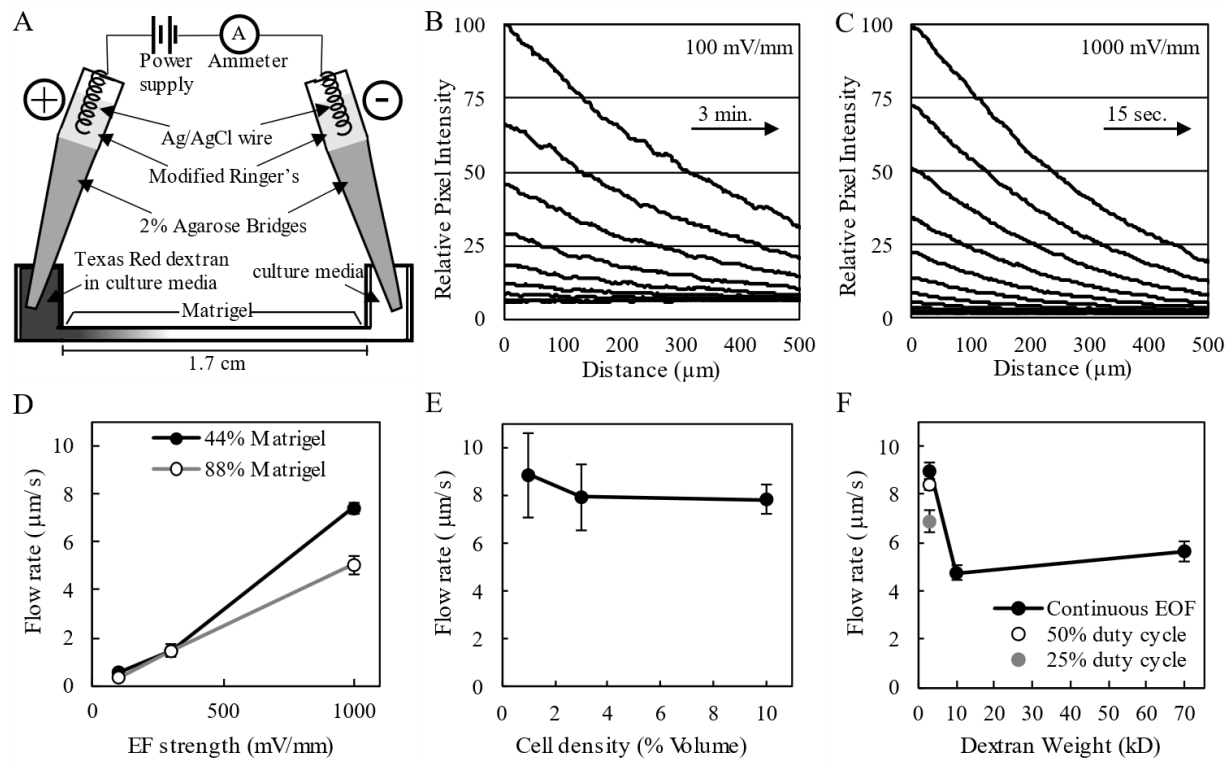


Figure 1. Electro-osmotic flow through Matrigel measured with neutral fluorescent dextrans. A. The experimental setup used to measure electro-osmotic flow through Matrigel filled IBIDI lanes included a power supply connected to the chamber via Ag/AgCl wires and 2% low EEO agarose bridges. Current was monitored using an ammeter in series and maintained by altering the applied voltage. B. The flow profile of 3kDa Texas Red dextran at 100 mV/mm is progressing from left to right. Flow profiles are shown at 3 min. intervals. C. The flow profile of 3kDa Texas Red dextran at 1000 mV/mm is progressing from left to right. Flow profiles are shown at 15 s intervals. D. EOF is dependent on EF strength and Matrigel density. Texas Red dextran (3 kDa) was used to measure EOF in Matrigel at three different field strengths. E. EOF is independent of cell concentration when cell density is $\leq 10\%$ by volume. F. Texas Red dextrans of 10 kDa and 70 kDa showed slightly lower velocities than EOF measured with 3 kDa dextran in 50% Matrigel. Monophasic pulsed EFs with a 50% duty cycle showed similar average flow velocity compared to continuous EFs but flow velocity during pulsed EFs with a 25% duty cycle was lower. Error bars represent S.E.M.

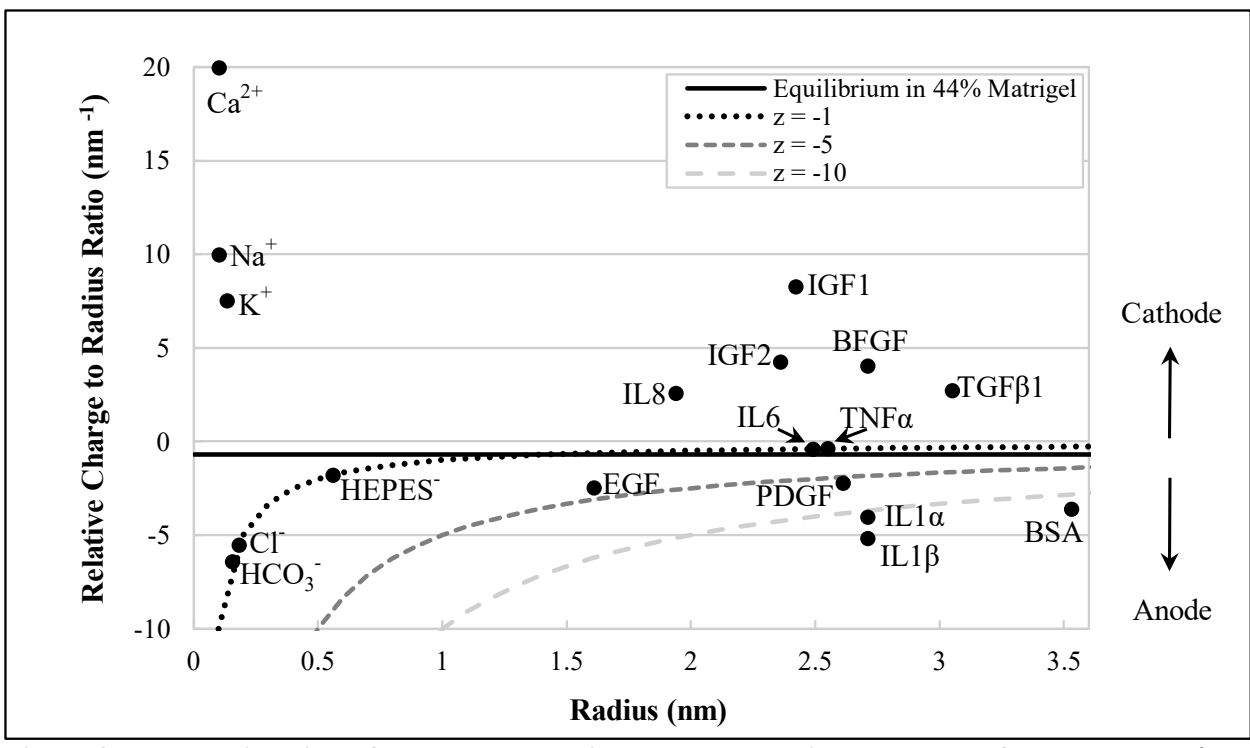


Figure 2. Electromigration of charged solutes is dependent on size and net surface charge. Solutes plotted above equilibrium between electrophoresis and electro-osmosis (solid black line) are predicted to migrate toward the cathode while solutes below the line are predicted to migrate toward the anode. Dotted and dashed lines illustrate the change in z/α ratio when the hydrodynamic radius of the solute increases and relative charge (z) remains constant. IGF – insulin-like growth factor, BFGF – basic fibroblast growth factor, TGFβ1 – transforming growth factor, EGF – epidermal growth factor, PDGF – platelet derived growth factor, IL1, IL6, IL8 – Interleukins 1, 6 & 8, TNFα - Tumor Necrosis Factor, BSA – bovine serum albumin, HEPES - anionic form of H⁺ buffer, Ca²⁺, Na⁺, K⁺, Cl⁻ HCO₃ - inorganic ions.

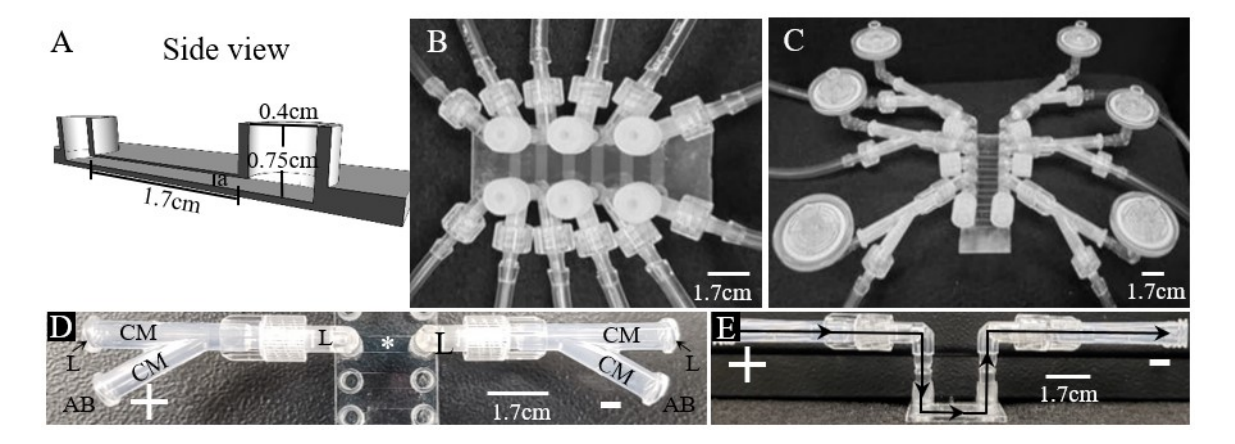


Figure 3. IBIDI chambers were used to induce interstitial flow through 3D cultures in Matrigel.

A. Illustration of a single IBIDI channel with dimensions of 0.04 cm deep (a), 0.38 cm wide and 1.7 cm long. **B**. Top view of PDP slide. PDP was generated through the channels by programmed compression of syringes connected to the channels using T-connectors and silicone tubing. Channels were drained using similar connectors and tubing (see also Fig. S1). **C**. Top view of EKP slide. EKP was applied to the channels using power supplies and Ag/AgCl electrodes connected to the channels by 2% low EEO agarose bridges (see also Fig. S2). Syringe filters (0.2 μm) were connected to the ends of culture media containing connectors to allow gas exchange and maintain aseptic conditions. **D**. Top view of partial EKP channel. Culture media (CM) is present in the L-connectors (L) and both branches of the Y-connector. Low EEO agarose bridges (AB) are connected to the angled branch. The asterisk marks the IBIDI channel containing cells and Matrigel, and the plus and minus symbols indicate electrical polarity. **E**. Side view of a magnified EKP channel. Black arrows show direction of fluid movement induced by an applied EF. Net fluid movement in the straight branches did not change height, preventing formation of pressure gradients.

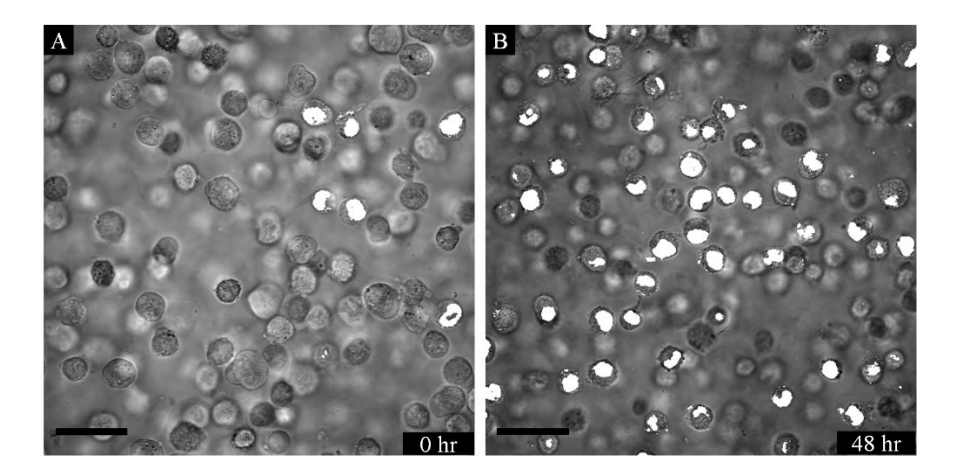


Figure 4. Propidium iodide stain of control cells in Matrigel filled channels. Images display overlays of PI fluorescence (pseudo-colored white) on the transmitted light images. A. After Matrigel crosslinking (0 hr.) a small fraction of cells show membrane disruption that allows PI staining. B. After 48 hr. in the absence of flow a significantly higher density of cells shows PI staining. Scale bar $-60 \mu m$.

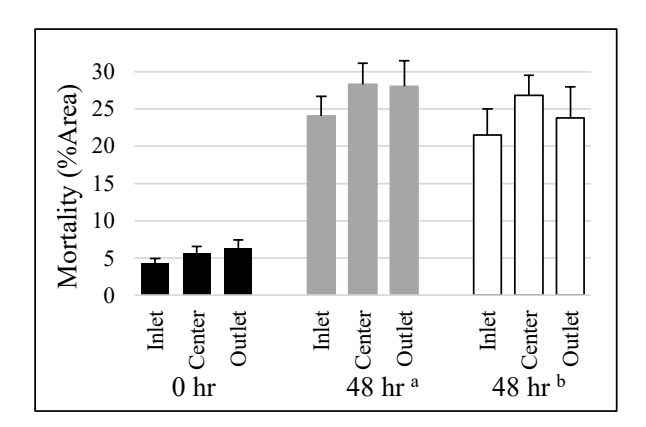


Figure 5. Cell mortality in 3D culture in the absence of interstitial flow. Propidium iodide staining was used to assess cell viability immediately after 3D culture of CHO cells and 48 hours later. ^a cultured in CO₂ incubator. ^b cultured on 37° C heating block and sealed from the atmosphere. Inlet and outlet for the nonperfused channels refer to the direction of perfusion during removal of transglutaminase and loading of PI.

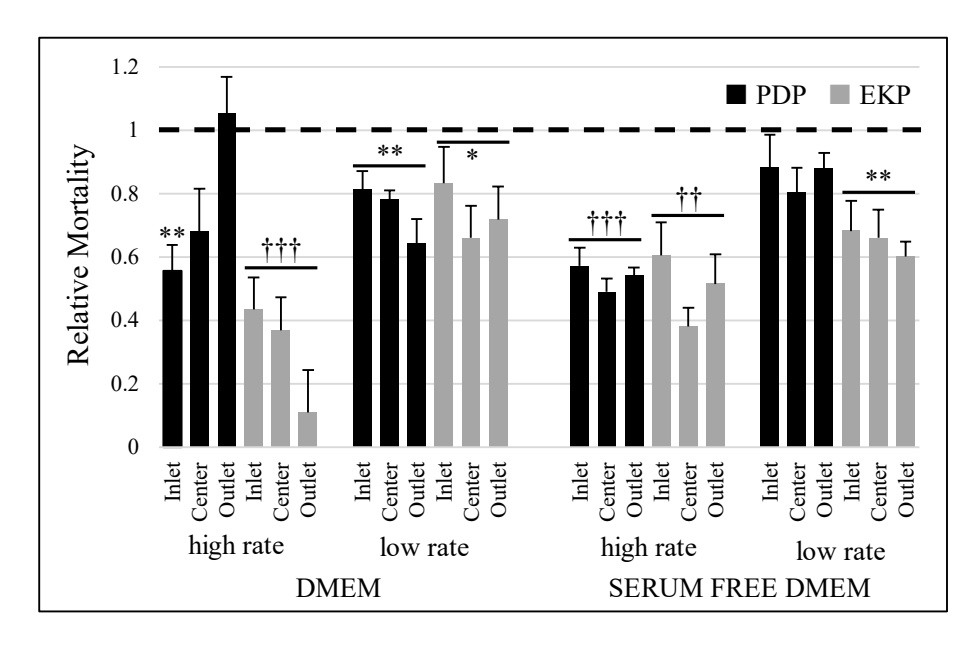


Figure 6. Perfusion most commonly reduces cell mortality in 3D culture. Relative mortality for PDP (black) and EKP (gray) were collected after 48 hr. at two different flow rates in DMEM culture media in the presence and absence of 10% serum containing growth factors. Symbols indicate p-values for the comparison between perfused conditions and nonperfused controls. * p < 0.05, ** p < 0.005, †† p < 0.001, ††† p < 0.0001.

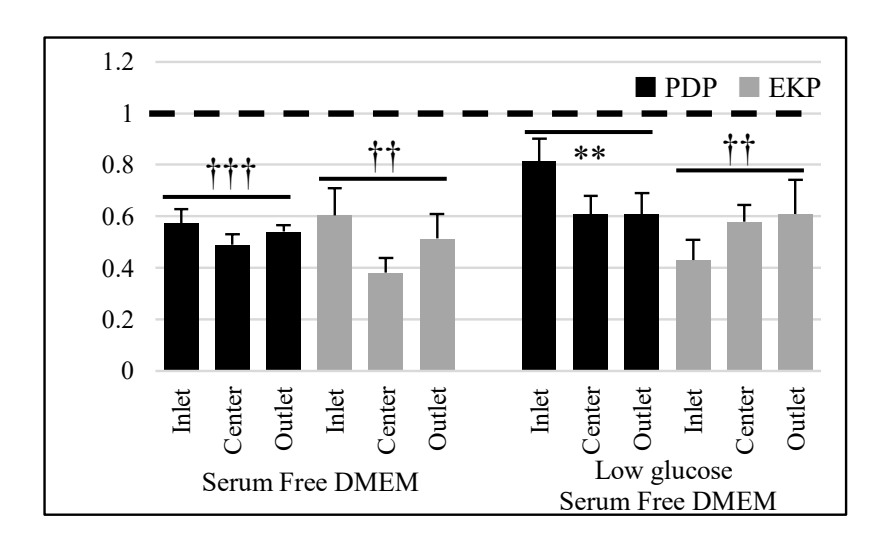


Figure 7. Lowered glucose does not significantly change viability in serum-free DMEM. Glucose reduction from 25mM to 5mM did not increase cell death in these 3D cultures. Symbols indicate p-values for the comparison between perfused conditions and nonperfused controls.

*** p < 0.005, †† p < 0.001, ††† p < 0.001.

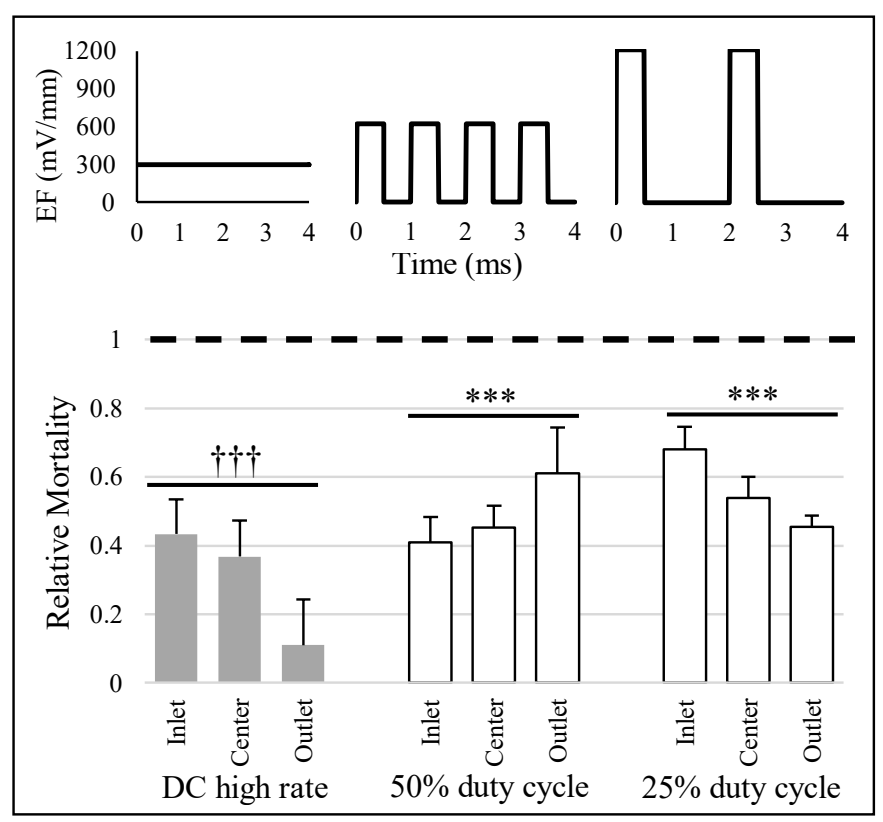


Figure 8. Time averaged EKP reduces mortality. Time averaged electric fields were maintained at 300 mV/mm for DC, and pulsed waveforms with 50% and 25% duty cycles. Waveform profiles are displayed above their relative mortality results. Reduction of mortality between DC and pulsed waveforms is not significantly different (p > 0.5 for both comparisons). Symbols indicate p-values for the comparison between perfused conditions and nonperfused controls. *** p < 0.0005, ††† p < 0.0001.

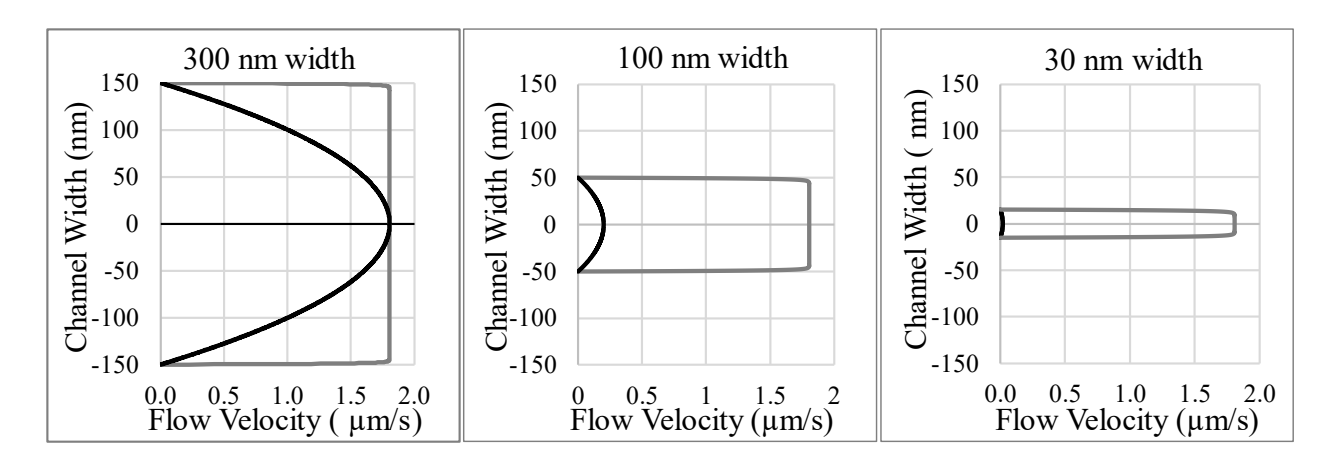


Figure 9. Modelled comparison of pressure driven flow and electro-osmotic flow through narrow planar channels. An applied pressure gradient of 1.2 mmHg/mm generates a parabolic flow profile (black) with peak flow of 1.8 μ m/s in the 300 nm channel, that decreases with distance between the two planes according to plane Poiseuille flow, i.e. 0.2 and 0.02 μ m/s for 100 and 30 nm distances. An applied EF of only 100 mV/mm through a channel with a -10 mV zeta potential, generates a plug profile (gray) in physiological saline with peak flow of 1.8 μ m/s for a range in distance between the walls. ²⁶

REFERENCES

- 1. Lovett M, Lee K, Edwards A, and Kaplan DL. Vascularization strategies for tissue engineering. Tissue Eng Part B Rev 2009;15:353-370.
- 2. Novosel EC, Kleinhans C, and Kluger PJ. Vascularization is the key challenge in tissue engineering. Adv Drug Deliver Rev 2011;63:300-311.
- 3. Swartz MA, and Fleury ME. Interstitial flow and its effects in soft tissues. Annu Rev Biomed Eng 2007;9:229-256.
- 4. Frykberg RG, and Banks J. Challenges in the treatment of chronic wounds. Adv Wound Care 2015;4:560-582.
- 5. Siemionow M, and Arslan E. Ischemia/Reperfusion injury: A review in relation to free tissue transfers. Microsurg 2004;24:468-475.
- 6. Elmore S. Apoptosis: A review of programmed cell death. Toxicol Pathol 2007;35:495-516.
- 7. Grilo AL, and Mantalaris A. Apoptosis: A mammalian cell bioprocessing perspective. Biotechnol Adv 2019;37:459-475.
- 8. Kroemer G, and Levine B. Autophagic cell death: the story of a misnomer. Nat Rev Mol Cell Bio 2008;9:1004-1010.
- 9. Park JY, White JB, Walker N, et al. Responses of endothelial cells to extremely slow flows. Biomicrofluidics 2011;5:022211.
- 10. Shi Z-D, Ji X-Y, Qazi H, and Tarbell JM. Interstital flow promotes vascular fibroblast, myofibroblast, and smooth muscle cell motility in 3-D collagen I via upregulation of MMP-1. Am J Physiol Heart C 2009;297:H1225-H1234.
- 11. McCarty WJ, and Johnson M. The hydraulic conductivity of MatrigelTM. Biorheology 2007;44:303-317.
- 12. Mattern KJ, Nakornchai C, and Deen WM. Darcy permeability of agarose-glycosaminoglycan gels analyzed using fiber-mixture and donnan models. Biophys J 2008;95:648-656.
- 13. Grimshaw PE, Grodzinsky AJ, Yarmush ML, and Yarmush DM. Dynamic membranes for protein transport: chemical and electrical control. Chem Eng Sci 1989;44:827-840.
- 14. Ou Y, Wu J, Sandberg M, and Weber SG. Electroosmotic perfusion of tissue: sampling the extracellular space and quantitative assessment of membrane-bound enzyme activity in organotypic hippocampal slice cultures. Anal Bioanal Chem 2014;406:6455-6468.
- 15. Kobylkevich BM, Sarkar A, Carlberg BR, et al. Reversing the direction of galvanotaxis with controlled increases in boundary layer viscosity. Phys Biol 2018;15:036005.
- 16. Sarkar A, Kobylkevich BM, Graham DM, and Messerli MA. Electromigration of cell surface macromolecules in DC electric fields during cell polarization and galvanotaxis. J Theor Biol 2019;478:58-73.
- 17. Graham DM, Huang L, Robinson KR, and Messerli MA. Epidermal keratinocyte polarity and motility require Ca²⁺ influx through TRPV1. J Cell Sci 2013;126:4602-4613.
- 18. Garcia AM, Frank EH, Grimshaw PE, and Grodzinsky AJ. Contributions of fluid convection and electrical migration to transport in cartilage: relevance to loading. Arch Biochem Biophys 1996;333:317-325.
- 19. Garcia AM, Szasz N, Trippel SB, Morales TI, Grodzinsky AJ, and Frank EH. Transport and binding of insulin-like growth factor I through articular cartilage. Arch Biochem Biophys 2003;415:69-79.
- 20. Rupert AE, Ou Y, Sandberg M, and Weber SG. Electroosmotic push-pull perfusion: Description and application to qualitative analysis of the hydrolysis of exogenous galanin in organotypic hippocampal slice cultures. ACS Chem Neurosci 2013;4:838-848.
- 21. Chen Y, Azad MB, and Gibson SB. Methods for detecting autophagy and determining autophagy-induced cell death. Can J Physiol Pharm 2010;88:285-295.
- 22. Walsh GM, Dewson G, Wardlaw AJ, Levi-Schaffer F, and Moqbel R. A comparative study of different methods for the assessment of apoptosis and necrosis in human eosinophils. J Immunol Methods 1998;217:153-163.

- 23. Maul GG, and Deaven L. Quantitative determination of nuclear pore complexes in cycling cells with differing DNA content. J Cell Biol 1977;73:748-760.
- 24. Han Y, Liu X-M, Liu H, et al. Cultivation of recombinant Chinese hamster ovary cells grown as suspended aggregates in stirred vessels. J Biosci Bioeng 2006;102:430-435.
- 25. Fox RW, and McDonald AT. Introduction to Fluid Mechanics. Fourth Edition ed. New York: John Wiley & Sons Inc.; 1992.
- 26. Soderman O, and Jonsson B. Electro-osmosis: Velocity profiles in different geometries with both temporal and spatial resolution. J Chem Phys 1996;105:10300-10311.
- 27. Miura T, and Tanaka R. *In vitro* vasculogenesis models revisited measurement of VEGF diffusion in Matrigel. Math Model Nat Pheno 2009;4:118-130.
- 28. Kihara T, Ito J, and Miyake J. Measurement of biomolecular diffusion in extracellular matrix condensed by fibroblasts using fluorescence correlation spectroscopy. PLOS ONE 2013;8:e82382.
- 29. Faraji AH, Cui JJ, Guy Y, Li L, and Weber SG. Synthesis and characterization of a hydrogel with controllable electroosmosis: A potential brain tissue surrogate for electrokinetic transport. Langmuir 2011;27:13635-13642.
- 30. Ng CP, and Swartz MA. Fibroblast alignment under interstitial fluid flow using a novel 3-D tissue culture model. Am J Physiol-Heart C 2003;284:H1771-H1777.
- 31. Ng CP, and Swartz MA. Mechanisms of interstital flow-induced remodeling of fibroblast-collagen cultures. Ann Biomed Eng 2006;34:446-454.
- 32. Pak SC, Hung SM, Bridges MW, Sleigh MJ, and Gray PP. Super-CHO-A cell line capable of autocrine growth under fully defined protein-free conditions. Cytotechnology 1996;22:139-146.
- 33. Rasmussen B, Davis R, Thomas J, and Reddy P. Isolation, characterization and recombinant protein expression in Veggie-CHO: A serum-free CHO host cell line. Cytotechnology 1998;28:31-42.
- 34. Kloth LC. Electrical stimulation technologies for wound healing. Adv Wound Care 2014;3:81-90.
- 35. Gardner SE, Frantz RA, and Schmidt FL. Effect of electrical stimulation on chronic wound healing: a meta-analysis. Wound Repair Regen 1999;7:495-503.
- 36. Messerli MA, and Graham DM. Extracellular electrical fields direct wound healing and regeneration. Biol Bull 2011;221:79-92.
- 37. McCarty WJ, Chimento MF, Curcio CA, and Johnson M. Effects of particulates and lipids on the hydraulic conductivity of Matrigel. J Appl Physiol 2008;105:621-628.
- 38. Zaman MH, Trapani LM, Sieminski AL, et al. Migration of tumor cells in 3D matrices is govered by matrix stiffness along with cell-matrix adhesion and proteolysis. P Natl Acad Sci USA 2006;103:10889-10894.
- 39. Leggio C, Galantini L, and Pavel NV. About the albumin structure in solution: cigar Expanded form versus heart Normal shape. Phys Chem Chem Phys 2008;10:6741-6750.
- 40. Krajewski A, Malavolti R, and Piancastelli A. Albumin adhesion on some biological and non-biological glasses and connection with their Z-potentials. Biomaterials 1996;17:53-60.
- 41. Dorh N, Zhu S, Dhungana KB, et al. BODIPY-based fluorescent probes for sensing protein surface-hydrophobicity. Sci Rep 2015;5:18337.
- 42. Meltzer H, and Silberberg A. Adsorption of collagen, serum albumin, and fibronectin to glass and to each other. J Colloid Interf Sci 1988;126:292-303.
- 43. Isseroff RR, and Dahle SE. Electrical stimulation therapy and wound healing: Where are we now? Adv Wound Care 2012;1:238-243.
- 44. Tagami H, Ohi M, Iwatsuki K, Kanamaru Y, Yamada M, and Ichijo B. Evaluation of the skin surface hydration in vivo by electrical measurement. J Invest Dermatol 1980;75:500-507.
- 45. Chizmadzhev YA, Indenbom AV, Kuzmin PI, Galichenko SV, Weaver JC, and Potts RO. Electrical properties of skin at moderate voltages: contribution of appendageal macropores. Biophys J 1998:74:843-856.
- 46. Denet A-R, Vanbever R, and Préat V. Skin electroporation for transdermal and topical delivery. Adv Drug Deliver Rev 2004;56:659-674.

- 47. Gomes RC, Guirro EC, Goncalves AC, Junior JAF, Junior LOM, and Guirro RR. High-voltage electric stimulation of the donor site of skin grafts accelerates the healing process. A randomized blinded clinical trial. Burns 2018;44:636-645.
- 48. Politis MJ, Zanakis MF, and Miller JE. Enhanced survival of full-thickness skin grafts following the application of DC electrical fields. Plast Reconstr Surg 1989;84:267-272.
- 49. Su T, Huang K, Mathews KG, et al. Cardiac stromal cell patch integrated with engineered microvessels improves recovery from myocardial infarction in rats and pigs. ACS Biomater Sci Eng 2020;6:6309-6320.
- 50. Noor N, Shapira A, Edri R, Gal I, Wertheim L, and Dvir T. 3D printing of personalized thick and perfusable cardiac patches and hearts. Adv Sci 2019;6:1900344.
- 51. Hamsher AE, Xu H, Guy Y, Sandberg M, and Weber SG. Minimizing tissue damage in electroosmotic sampling. Anal Chem 2010;82:6370-6376.
- 52. Rupert AE, Ou Y, Sandberg M, and Weber SG. Assessment of tissue viability following electroosmotic push-pull perfusion from organotypic hippocampal slice culture. ACS Chem Neurosci 2013;4:849-857.
- 53. Tung L, Sliz N, and Mulligan MR. Influence of electrical axis of stimulation on excitation of cardiac muscle cells. Circ Res 1991;69:722-730.

SUPPLEMENTAL INFORMATION

Electrokinetic Perfusion Through 3D Culture Reduces Cell Mortality

Anyesha Sarkar¹ and Mark A. Messerli PhD¹

¹Department of Biology and Microbiology, South Dakota State University, Brookings, SD, 57007

Additional Materials and Methods

Experimental setup for electro-osmotic flow measurements

EOF through Matrigel was measured by casting Matrigel mixed with transglutaminase into IBIDI lanes. Texas Red dextrans, 3 or 10 or 70 kDa, mixed with culture media was added to the anode well at a final concentration of 20 μ M while the other well was filled with an equal volume of culture media. Ag/AgCl electrodes were immersed in modified Ringer's (MR) and connected to the IBIDI wells with 2% low EEO agarose bridges (Fisher Scientific, Waltham, MA) containing MR. The electrodes were connected to a power supply and the average current density was maintained by monitoring current with an ammeter in series and adjusting the applied voltage. Time-lapse images of the dye front were recorded at 4, 2 and 1 frame(s)/min for EFs of 1000, 300 and 100 mV/mm, respectively, until the dye had travelled ~750 μ m. Images were also collected between EOF experiments in the absence of EFs to track EOF independent migration.

Experimental setup for 3D viability assays

CHO cells were cultured in crosslinked Matrigel by allowing cells to settle to the bottom of a sterile tube in MR before collecting a volume of the concentrated cells and mixing with Matrigel stock to make their final volumes in the mixture as 40% and 50%, respectively. Microbial transglutaminase was added to make up the final 10% volume of the mixture. This mixture was then loaded into IBIDI channel slides and allowed to gel as described previously. PDP was applied using syringe pumps connected to IBIDI slides with T-connectors or L-connectors and silicone tubing, Fig. S1A. A protective 1% agarose gel was added to the inlet well of both perfused and control lanes to prevent the gel from being dislodged from the IBIDI

lane during application of fluid pressure. T or L-connectors were added to the inlet side of the lanes after the agarose had gelled. Syringe pumps were fitted with 3mL syringes filled with CO₂-equilibrated sterile culture media. T-shaped connectors, Fig. S1B, were fitted on both wells of the perfused lanes and L-shaped

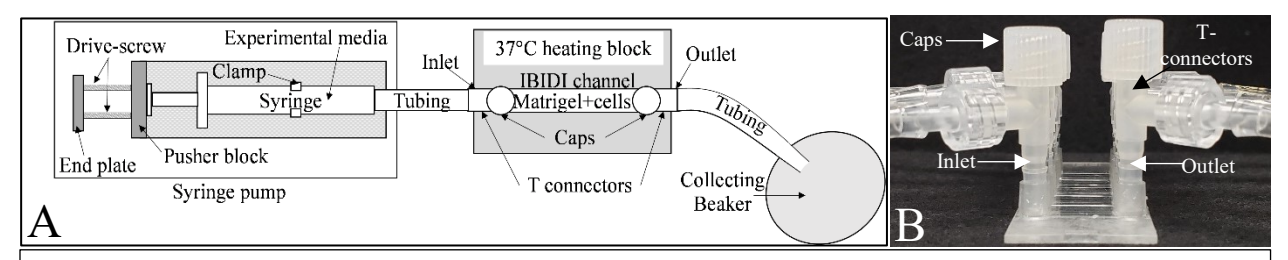


Figure S1. Experimental setup of perfused lanes for PDP. A. Illustration shows the top view of an IBIDI channel fitted to a programmable syringe pump to deliver PDP. B. Side view of a magnified PDP channel. T-connectors on both sides are sealed with caps after filling them with experimental media.

connectors were fitted to the control lanes. After the T-shaped connectors were joined to the syringe by tubing they were filled with media and capped. The L-shaped connectors were filled and fitted to the control syringes. IBIDI channel outlets were drained into a collecting beaker via tubing, Fig. S1A. Cells and IBIDI chambers were maintained at 37°C using a temperature-controlled heating block. The 37°C heating block was used during PDP to protect the syringe pumps from the heat and humidity of the CO₂ incubator while keeping the silicone tubes short.

EKP was generated using power supplies connected to IBIDI channels using Y-connectors in-line with L-connectors, Fig. S2. The straight branch of the Y-connectors supplied culture media. Air exchange occurred through 0.2 μm syringe filters to maintain aseptic conditions. EFs were applied through 2% low

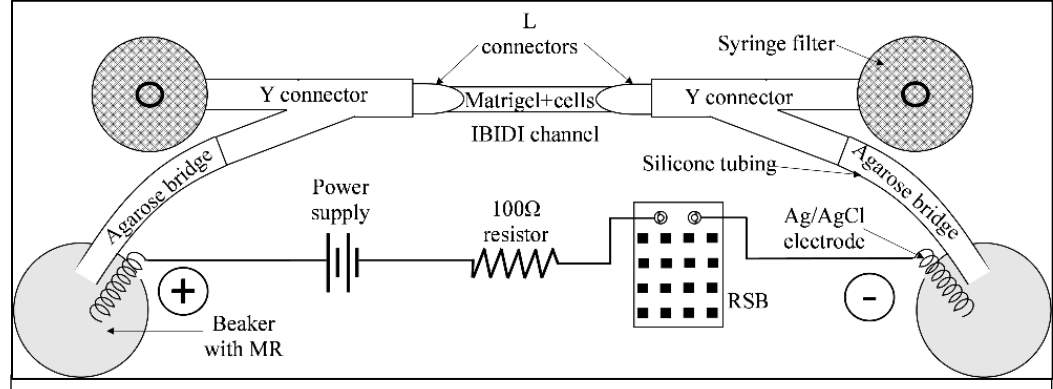


Figure S2. Top view of the experimental setup for an EKP channel. RSB: Resistance Substitution Box. MR: Modified Ringer's

EEO agarose bridges connected to the angled branch of the Y-adapter, Fig. S2. This arrangement of

connectors prevented a change of net fluid height and buildup of back pressure. The low EEO agarose bridges in culture media were formed in silicone tubing (9 cm long) that joined the Y-connectors to the power supplies through Ag/AgCl electrodes immersed in MR contained in small beakers. Electrodes were connected to power supplies using a resistance substitution box in series for each circuit. The EF across the circuit was maintained by repeatedly checking the voltage drop across a known 100-ohm resistor connected in series between the power supply and the resistance substitution box. In the absence of EFs, channels were sealed on both ends with ~650 µL of media in wells and L-connectors, i.e. greater than 21 times the volume of the cell loaded channel, on both sides. Chambers were kept in a 37°C CO₂ incubator for the duration of the experiment and media was replaced on each side of the perfused channels and in the Ag/AgCl electrode baths every 12 hours.